Article

Modeling of an Industrial Vibrating Double-Deck Screen of a Urea Granulation Circuit

Ivana M. Cotabarren, Jose# Rossit, Vero#nica Bucala#, and Juliana Pin#a

Ind. Eng. Chem. Res., **2009**, 48 (6), 3187-3196• DOI: 10.1021/ie800968y • Publication Date (Web): 17 February 2009

Modeling of an Industrial Vibrating Double-Deck Screen of a Urea Granulation Circuit

Ivana M. Cotabarren,* José Rossit, Verónica Bucalá, and Juliana Piña

Department of Chemical Engineering, PLAPIQUI, Universidad Nacional del Sur, CONICET, Camino La Carrindanga Km. 7, (8000) Bahía Blanca, Argentina

A reliable mathematical model to predict the performance of double-deck screens from an industrial urea granulation circuit is provided in this work. The classification in each deck was described by the empirical model reported by Karra [Karra, V. K. Development of a Model for Predicting the Screening Performance of a Vibrating Screen. *CIM Bull.* 1979, *72*, 804.] for the mining industry. The estimation of model parameters was based on industrial data collected from two large-scale double-deck screens belonging to a urea granulation plant. Prior to parameter fitting, data reconciliation of the solid streams was performed, with the aim of determining the unmeasured mass flows and the reconciled particle size distributions that fulfill the material balances for every size class. The results indicate that the fitted model reproduces in an accurate way the performance of the urea granules classification device. Thus, the screen mathematical representation can be used as a module of a plant simulator for many existing urea granulation circuits, which (independently of the technology) have similar industrial vibrating double-deck screens to attain the marketable product granulometry. In addition, the fitted model allows finding the optimal screen apertures to achieve the desired product attributes and recycle ratios.

1. Introduction

Granulation is a key particle size enlargement process, widely used in the pharmaceutical, food, mining, and fertilizer industries.[2−4] Approximately 60% of the products in the chemical industry are produced in granular form,[5] and thus granulation constitutes a very important process to be fully understood. Granulation converts fine particles and/or sprayable liquids (suspensions, solutions, or melts) into granular material with more desirable properties than the original feed.

The granulation process is considered as one of the most significant advances in the fertilizers industry, providing products with high strength and low tendency to caking and lump formation. The global market conditions for agricultural commodities have been exceptionally favorable since the first half of 2007; the associated global fertilizer demand sharply increased (+5%) in 2006/2007. In response to strong market fundamentals, world demand is expected to further expand. Among the nitrogenous fertilizers, the urea capacity was forecasted to grow from 136 Mt in 2008 up to 192 Mt in 2011.[6]

Urea granulation is a complex operation that cannot be carried out in a single device. It is rather achieved by a combination of process units with specific functions constituting a granulation circuit (Figure 1).[7] The main unit is the granulator where small urea particles, known as seeds (generally out of specification product), are continuously introduced and sprayed with a concentrated solution of the fertilizer (melt). The seeds grow through deposition of the melt droplets onto the solids surface, followed by urea solidification and water evaporation.[8] The granules that leave this size enlargement unit are cooled down and subsequently classified by double-deck screens into product, oversize, and undersize streams. The product is transported to storage facilities, while the oversize fraction is fed to crushers for size reduction. The crushed oversize particles are then combined with the undersize granules and returned to the granulator as seeds.[9]

Generally, in fertilizer granulation plants, only a relatively small fraction of the material leaving the granulator is in the specified product size range. Therefore, high recycle ratios are common. The characteristics of the recycle, which are a consequence of what happened previously in the granulator, screens, and crushers, influence what will happen a posteriori in the size enlargement equipment. Thus, cycling surging and drifting of particles might take place. In extreme cases, these periodical oscillations coupled with large dead times can result in plant shutdown or permanent variations in the plant capacity as well as product quality.[2,10] To minimize these problems, it is necessary to have a fundamental understanding of the effects of recycling material on the circuit behavior.

Many authors found that the operation of the screening and crushing units has a decisive influence on the recycle stream and hence on the circuit stability.[5,10−13] In view of this and the recognized important role of plant simulation to predict and optimize the granulation circuit operation,[2,12−14] reliable models for all the process units should be available. There are many plants of urea granulation spread around the world which are mainly operated by trial and error. The urea world installed capacity and the forecasted growth for the urea market indicate the need to focus research on urea granulation circuits to improve the efficiency of the plants in order to increase their competitiveness.

Recently, a validated mathematical model for industrial double-roll crushers of a urea granulation circuit has been reported.[9] As for the crushers, the screens' modeling requires the knowledge of some parameters that have to be fitted from experimental data.

Screening is probably the oldest and most widely used physical size separation method in industrial operations for continuous classification of solid streams. The employment of screens has spread to a variety of engineering categories, from the traditional mining sector to the contemporary fast-growing food and pharmaceutical engineering.[15] The fertilizer industry

* To whom correspondence should be addressed. Tel: 54-291-486-1700, ext 270. Fax: 54-291-486-1600. E-mail: icotabarren@plapiqui.edu.ar.

10.1021/ie800968y CCC: $40.75
Published on Web 02/17/2009

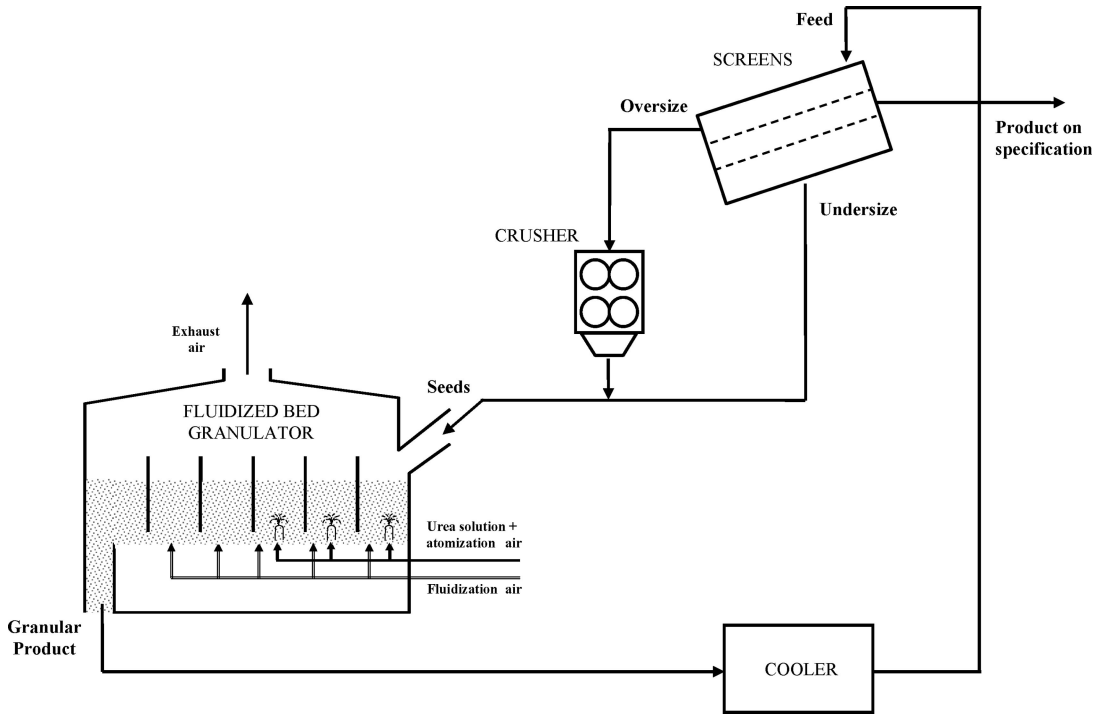

Figure 1. Typical urea granulation circuit.

requires, as aforementioned, a classification step that is usually performed by double-deck vibrating screens.

Vibrating screens have been extensively studied by numerous authors in the context of the mining processing industry.[1,16−20] Models in the literature can be classified as phenomenological, empirical, and numerical, being based on theory of the screening process, empirical data, and computer solutions of Newtonian mechanics, respectively.[21]

Within the phenomenological models two different approaches, the kinetic and probabilistic, have been used to represent these screening operations. The probabilistic approach[16,18] is based on the probability of a particle passing through the aperture of the screen. On the other hand, the kinetic approach defines the screening performance as a rate process that varies with the distance along the screen and depends on the amount and particle size distribution of the material being processed. According to Ferrara et al.[17] a zero-order process occurs at the beginning, while as the quantity of material on the screen declines, a first-order process takes place. Subasinghe et al.[19] described the screening operation by an alternative approach, which uses two first-order rate processes. Soldinger[20] established that the screening process involves two mechanisms, stratification and passage of particles through the screen apertures. The rate of stratification varies with the proportion of fine material and the particle sizes, while the rate of passage depends on the probability that the particles will pass through the apertures as well as the amount of fine material on the screen surface. This last mechanism could be considered as a combination of the kinetic and probabilistic approaches.

The empirical models aim to predict the quantity of undersize that can pass through the screen based on a theoretical capacity. This base capacity is affected by a set of correction factors which account for, among others, the effect of oversize, half-size, and near-size material. Other correction factors include whether the screen is a top or lower deck on a multideck unit, type of aperture, material density, etc.[21] Due to their simplicity, the empirical models are preferred for the simulation of industrial screens. In fact, many commercial simulators such as Aspen Plus,[22] Modsim,[23] and Moly-Cop Tools[24] have empirical models implemented in their routines.

In relation to the fertilizer industry, Adetayo[25] and Wildeboer[14] adapted the probabilistic model reported by Whiten[16] to represent vibrating screens present in granulation circuits. With the same purpose, Heinrich et al.[10] modified the Molerus and Hoffman[26] classification function, formerly developed for cyclones.

In this contribution, a fitted model for a large-scale double-deck vibrating screen based on industrial data of a urea granulation plant is presented. Prior to adjusting the screen model, all the flow rates around the equipment and their corresponding particle size distributions must be known. It is common knowledge that significant errors may occur when attempting to measure solid stream flow rates. In fact, the only reliable and available experimental mass flow for this work was that corresponding to the product stream. The remaining and unmeasured individual mass flows were determined through a data reconciliation procedure, which simultaneously allows modifying the most unreliable measured variables to satisfy the material mass balances for every size class.[5,27]

The screen mathematical model proposed by Karra[1] (usually recommended for predicting the performance of industrial vibrating screens[28]) was found, after thorough discrimination of several empirical, probabilistic, and kinetic models, as the most suitable one to reproduce the available industrial data.

2. Industrial Data

In the present work, the screen classification parameters were fitted using industrial data from a plant of high capacity. The experimental data were collected from two large-scale double-deck vibrating screens of identical characteristics. They operate with a small angle of inclination and with fixed vibration. Samples by duplicate of the feed (F) and of the oversize (O), product (P), and undersize (U) streams of each of the two screens (A and B) were collected and granulometrically analyzed every 4 and 12 h for two independent experiments (tests 1 and

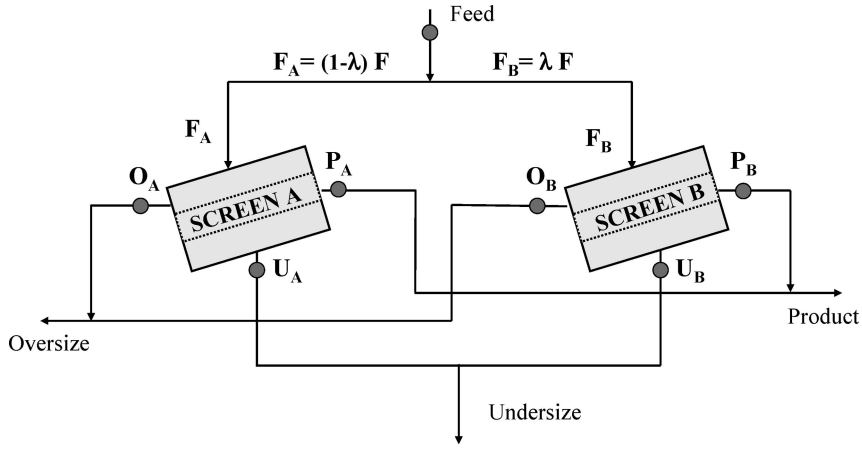

Figure 2. Schematic diagram of the experimental screening sector. (●) Sampling points.

2) that lasted 36 and 78 h, respectively (Figure 2). During these plant experiments just the distance between the rolls of the downstream crushers were modified; the remaining operating variables of the whole circuit were kept constant. Obviously, this change in the crusher operating conditions had a direct effect on the recycle to the granulator, and hence, affected the feed (F) to the screens and modified their performance.

The sampling was carried out manually following the guidelines given by Allen.[29] The feed and oversize were sampled from the free-falling streams entering to the screens and crushers, respectively. The undersize was sampled from the free-falling stream exiting the screens lower deck before being combined with the crushed oversize fraction. The sample cutters were always moved across the entire streams at right angles (i.e., perpendicular to the stream directions), in regular intervals and with relatively constant speed. The product stream was sampled from the conveyor belts to storage facilities; the whole of the particles were collected intermittently by a scoop on a short length of the belt. All the samples were placed in labeled sealed bags. The collected samples were reduced to laboratory samples with a chute splitter. The corresponding particle size distributions were determined by the dry sieving method at constant sieving times and agitation rates. A stack of 13 stainless steel sieves and a mechanical sieve shaker were used for the analysis. The undersize mass flow was continuously measured. However, as usually happens in so many industrial plants, gross errors were detected in this measurement. Therefore, and as aforementioned, the only available and reliable mass flow rate around the screens was the one corresponding to the product (P) stream. Thus, to fit the double-deck screen model, the calculation of the total feed (F) and its split substreams (F_A and F_B), the oversize (O), and undersize (U) streams was necessary. To compute these flow rates and fulfill the material balances for every size class, the industrial data reconciliation was first performed.

3. Data Reconciliation

Data reconciliation was formulated as a constrained optimization problem and solved by means of the Athena Visual Studio software.[30] The goal of this optimization problem was to minimize the total difference between measured and estimated mass fractions for each size class, weighted by the variance of the measurements using the least-squares method.[27] The objective function was expressed as

$$f_o = \sum_{j=1}^{M}\sum_{i=1}^{N}\frac{(X_{ji} - \overline{X_{ji}})^2}{W_{ji}} \quad (1)$$

where N is the number of size classes (i.e., 13) and M is the number of streams around the screens with different particle size distributions (i.e., 7: O_A, P_A, U_A, O_B, P_B, U_B, and F, since F_A and F_B have the same mass fractions). $\overline{X_{ji}}$ represents the average value of the mass fractions for stream j and the size class i. X_{ji} corresponds to the reconciled mass fractions and W_{ji} is the variance associated with each $\overline{X_{ji}}$.

To completely formulate the data reconciliation, the objective function (f_o) was subjected to the following restrictions:

$$\begin{aligned} F_A X_{F_A i} &= O_A X_{O_A i} + P_A X_{P_A i} + U_A X_{U_A i} \\ F_B X_{F_B i} &= O_B X_{O_B i} + P_B X_{P_B i} + U_B X_{U_B i} \end{aligned} \quad (2)$$

$$\sum_{i=1}^{13} X_{ji} = 1 \quad j = 1,...,7 \quad (3)$$

$$P_A + P_B = P \quad (4)$$

$$\frac{F_A}{1-\lambda} = \frac{F_B}{\lambda} \quad (5)$$

where λ is the fraction of the total feed derived by a diverter to screen B (Figure 2). P corresponds to the measured product flow rate, which was not a variable to be reconciled. The diverter position was manually fixed to equally distribute the feed to both screens. Nevertheless, an exactly equal distribution was not guaranteed.

Figure 3 condenses the correspondence between the reconciled and experimental mass fractions for each particle size and solid stream. The observed differences are as expected, considering the well-known uncertainties when sampling and analyzing solid streams. Indeed, from the 1638 total experimental points (test 1: 13 size classes × 7 streams × 10 samples; test 2: 13 size classes × 7 streams × 8 samples), 92% are included within the 20% deviation lines, and 81% within the 10% lines.

The feed flow split parameter (λ) varied from 0.43 to 0.56, with its average value being 0.48. These results indicated that the diverter was almost capable to split the feed evenly. The feed flow rates (F) estimated through the reconciliation procedure were in good agreement with the values calculated from the energy balance of the cooler located downstream from the granulation unit. The reconciliation step was essential to have consistent industrial experimental data to fit the screen models.

4. Screen Model

As is well-known, screen separation depends on the probability that particles smaller than the aperture size reach the

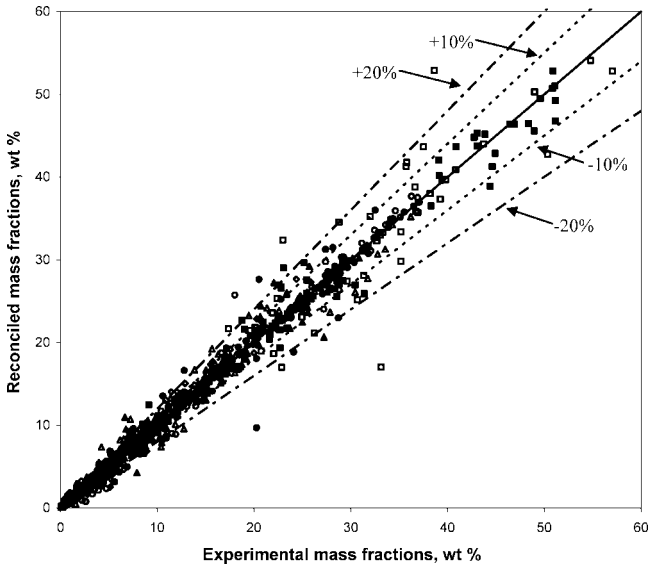

Figure 3. Reconciled vs experimental mass fractions of all the size classes. Test 1: (◆) F, (■) O_A and O_B, (▲) P_A and P_B, and (●) U_A and U_B. Test 2: (◇) F, (□) O_A and O_B, (△) P_A and P_B, and (○) U_A and U_B.

screen and pass through it.[31] A screen with an ideal performance would separate all the undersize material. However, separation processes are not perfect and the probabilities of reaching the screen and passing through it are not the same for different particle sizes.

The most realistic measurement of screen performance is provided by the partition curves. To represent a nonideal classification operation, like the urea screening process, oversize partition coefficients for each size class can be used. For each class size i, the oversize partition coefficient (T_i) is defined as the amount of oversize within class i divided by the amount of material of that size in the feed.

$$T_i = \frac{OX_{Oi}}{FX_{Fi}} \tag{6}$$

Once all T_i values are known, the particle size distributions of the oversize and undersize streams can be calculated through simple mass balances for the solids belonging to each size class i.

$$OX_{Oi} = T_i FX_{Fi} \tag{7}$$

$$UX_{Ui} = (1 - T_i)FX_{Fi} \tag{8}$$

The oversize partition values (T_i) are usually plotted against the corresponding geometric mean particle size:

$$d_i = \sqrt{(d_1 d_2)_i} \tag{9}$$

where d_1 and d_2 are the lower and upper limits for size class i, respectively.

Figure 4 shows the real partition curve against a screen with ideal performance. In order to develop an empirical model capable of describing the screening behavior, a mathematical formulation of the partition curve is needed. The partition coefficients are function of either the screen aperture or the d_{50} parameter. The d_{50} cut size is defined as the size corresponding to the 50% partition curve, and thus represents the size at which particles have equal chance of staying on the screen or passing through it (Figure 4). The cut size is a measure of the screening efficiency; d_{50} values close to the mesh size indicate high

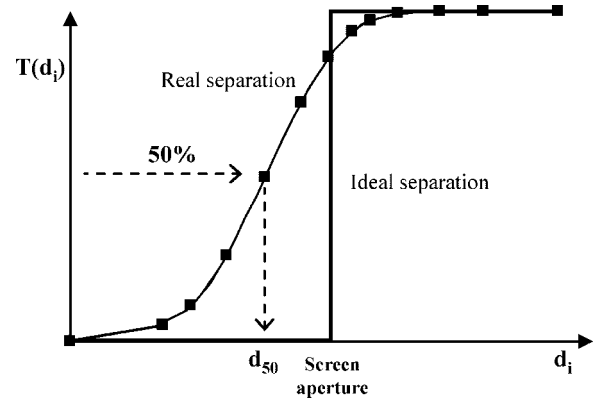

Figure 4. Oversize ideal and real partition curve.

efficiencies. The available industrial data indicated, as frequently happens,[21] that the cut sizes were lower than the corresponding mesh apertures (h) for all the experiments.

Several screens models were evaluated in order to determine the best option for describing the urea granulation data. Most of the kinetic models reported in the open literature[17,19,20] are based on the adjustment of parameters that depend on the ratio d_i/h instead of d_i/d_{50}. Consequently, the partition curve (T_i) becomes equal to 1 for all the particles having sizes greater than the screen aperture, indicating that they will remain over the screen. This is only true for perfectly spherical particles. Real operations do not handle perfectly spherical solids, and thus particles with one dimension smaller than the aperture pass through it provided they approach the screen surface at an adequate angle. Therefore, neither of these models was adequate to represent correctly the acquired plant data. Adetayo[25] and Wildeboer[14] adopted the Whiten[16] probabilistic model, which considers the probability of passing through for particles in the ith size class a function of the d_i/h ratio. For this reason, the Adetayo[25] and Wildeboer[14] models were also improper to describe the industrial data. The Heinrich et al.[10] probabilistic model included a classification function in terms of a constant d_{50} (i.e., independent of operating and material conditions). However, it has been established that process variables such as particle to aperture ratio, composite nature of the feed, deck location, feed rate, and bulk density, affect d_{50}.[1] The influence of these variables on the cut size values was confirmed for the acquired urea data. Hence, the Heinrich et al.[10] model was not appropriate either. The empirical model proposed by Karra[1] became the overwhelming one, among all the tested mathematical representations, because the cut size rather than being constant is calculated as a function of process variables. This author proposed the following d_{50} correlation to represent industrial screening data:

$$d_{50} = h\left(\frac{U^T/S}{K}\right)^a \tag{10}$$

where h is the screen aperture and U^T is the theoretical undersize mass flow fed to the screen (fed material whose size is smaller than the aperture size). S is the screen surface, K is a product of factors that correct the screen basic capacity, and a is a fitting parameter.

The variable K is expressed as follows:

$$K = ABCDEF_D G \tag{11}$$

where A is the basic capacity, defined as undersize mass flow that a particular screen can process per unit of screen area. B is

Table 1. Equations for Screen Correction Factors[1]

factor	equation	
A	$A = 12.1286h^{0.3162} - 10.2991$	$h < 50.8$ mm
	$A = 0.3388h + 14.4122$	$h \geq 50.8$ mm
B	$B = -0.012Q + 1.6$	$Q \leq 87$
	$B = 0.0425Q + 4.275$	$Q > 87$
C	$C = 0.012R + 0.7$	$R \leq 30$
	$C = 0.1528R^{0.564}$	$30 < R < 55$
	$C = 0.0061R^{1.37}$	$55 \leq R < 80$
	$C = 0.05R - 1.5$	$R \geq 80$
D	$D = 1.1 - 0.1L$	
E	$E = 1.0$	$T < 1$
	$E = T$	$1 \leq T \leq 2$
	$E = 1.5 + 0.25T$	$2 < T < 4$
	$E = 2.5$	$4 \leq T \leq 6$
	$E = 3.25 - 0.125T$	$6 < T \leq 10$
	$E = 4.5 - 0.25T$	$10 < T < 12$
	$E = 2.1 - 0.05T$	$12 \leq T \leq 16$
	$E = 1.5 - 0.125T$	$16 < T < 24$
	$E = 1.35 - 0.00625T$	$24 \leq T \leq 32$
	$E = 1.15$	$T > 32$
F_D	$F_D = \rho_B/1602$	
G	$G = 0.975(1 - X^{0.511})$	

the amount of oversize in the feed (percentage of material with $d_i > h$). Screens that handle a great amount of oversize operate more efficiently because that material is directly recovered over the screen. C is the amount of half-size under in the feed (percentage of material with $d_i < 0.5h$). Feeds containing a large proportion of material considerably smaller than the aperture size can be handled more easily by the screen. D is the location of the deck. Lower decks receive material harder to handle than those decks that take fresh feeds; therefore, the capacity decreases with position. E is for wet screening. If dry screening is performed, as in the urea process, its value is set to one. F_D is the bulk density factor; denser materials are separated more easily than lighter materials. G is the amount of near-size material in the feed (percentage with material of $0.75h < d_i < 1.25h$). Feeds with large quantities of particles close to the aperture size present more difficult separation because the passage of undersize material is inhibited.[31]

Karra[1] used the standard expressions given in the Nordberg Process Machinery Reference Manual[32] for parameters A, B, C, D, E, and F_D and developed his own correlation for the near-size material factor G. The corresponding equations are presented in Table 1.

Once d_{50} is determined, its relationship with the T_i function has to be defined. Several standard functional forms are available to describe it; Karra[1] proposed

$$T_i = 1 - \exp\left(-0.693\left(\frac{d_i}{d_{50}}\right)^m\right) \tag{12}$$

This correlation, recognized as the Plitt equation, is expressed in terms of the well-known Plitt's adjustable parameter m, which defines the classification sharpness.[33]

5. Parameter Estimation

Each deck of the industrial classification device was considered as a separate screen; therefore, a set of parameters was adjusted for the top deck and another for the bottom one. Following the procedure described in the previous section, the correction factors A to G were determined for both decks using the expressions given in Table 1. The screen factor E, corresponding to wet screening, was equal to 1.

For the special case under consideration, the bulk density corresponding to each industrial deck was not a measurable property because it varied along the screen length with the quality of the material being classified. For this reason, it was set as a fitting parameter for both decks.

Once the theoretical undersize U^T and all the correction parameters that defined K were evaluated for each test hour and deck, the d_{50} were calculated by means of eq 10 and the corresponding partition coefficients curves were constructed.

The adjustment of the bulk density (ρ_B), the Plitt parameter (m), and the exponent in d_{50} (a) for each deck was performed by using the Athena Visual Studio software[30] with the aim of reproducing the respective cumulative undersize and oversize streams. The undersize from the top deck was considered as the feed to the bottom one.

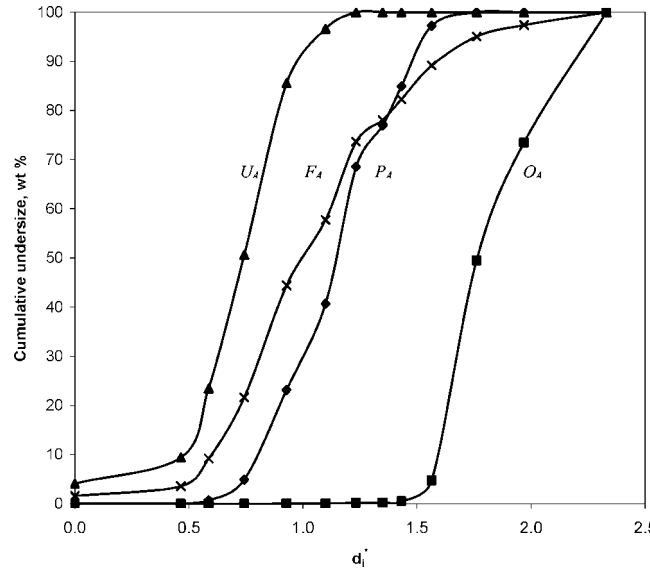

Figure 5. Typical experimental screen A performance.

Table 2. Estimated Parameters for the Top and Bottom Deck Screens

parameter	top deck	bottom deck
bulk density, ρ_B (kg/m^3)	560	705
power of d_{50} equation, a	−0.0023	−0.2862
Plitt's parameter, m	25.097	3.758

6. Results

The typical overall performance of the studied large-scale double screen, in terms of cumulative mass particle size distributions, is shown in Figure 5. Table 2 reports the estimated model parameters. The fitted values are in agreement with the usual operation of both decks. In fact and due to the greater amount of oversize material (i.e., higher bed porosity), the bulk density for the top deck is lower than the one corresponding to the bottom deck. The solid urea density is 1330 kg/m^3, so the bulk densities found for the top and bottom decks indicate bed porosities of about 58% and 47% respectively. The separation sharpness as a function of the feed quality is clearly represented through the adjusted Plitt parameter. The top deck handles material with a greater proportion of oversize than the bottom deck, being more effective in the classification process. One way of quantifying the deviation from perfect separation is to determine the Ecart probability (E_p), or probable error, defined as[34]

$$E_p = \frac{d_{75} - d_{25}}{2} \tag{13}$$

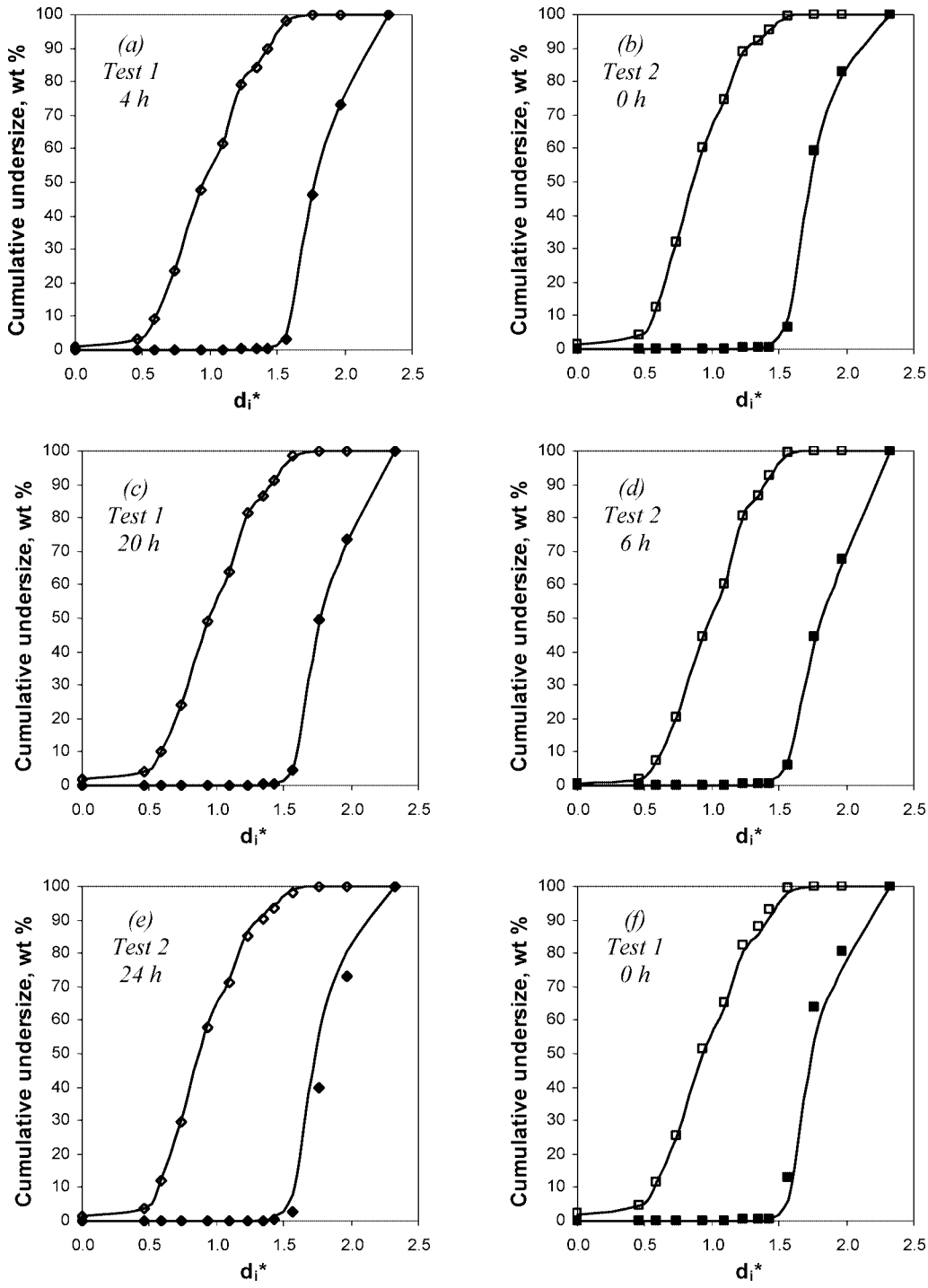

Figure 6. Some selected experimental and predicted size distributions for the top deck. Screen A: (◆) experimental oversize, (◇) experimental undersize, and (□) predicted. Screen B: (■) experimental oversize, (□) experimental undersize, and (—) predicted.

where d_{75} and d_{25} are the particle sizes for which the partition coefficients are equal to 0.75 (or 75%) and 0.25 (or 25%), respectively.

As the slope of the partition curves approaches the vertical, the probable error tends to zero (i.e., the smaller the probable error, the closer the screen performance becomes to a perfect separation).[34] The calculated average E_p values for the top and bottom decks were 0.21 and 0.46. Thus, the higher efficiency of the first deck, given by a significant higher m value, is confirmed.

The exponent in the d_{50} correlation (a) can be considered as an indicator of the cut size evolution during the operation. According to the fitting results, the d_{50} for the top deck remains close to the screen aperture (see eq 10). This result is in agreement with the higher efficiencies found for this first deck. Contrarily, the d_{50} for the bottom deck is a strong function of the operating conditions and differs considerably from the corresponding h value. Indeed, the highest d_{50}/h ratio over time obtained for the top deck was 0.4% against 31.9% for the bottom one.

Figure 6 shows the experimental and calculated oversize (O) and undersize ($U + P$) particle size distributions (PSDs) for the top deck. Three samples from screen A (Figure 6, a, c, and e) and three from screen B (Figure 6, b, d, and f), among the 36 acquired, have been included in order to illustrate the goodness of the model. The samples presented in Figure 6, e

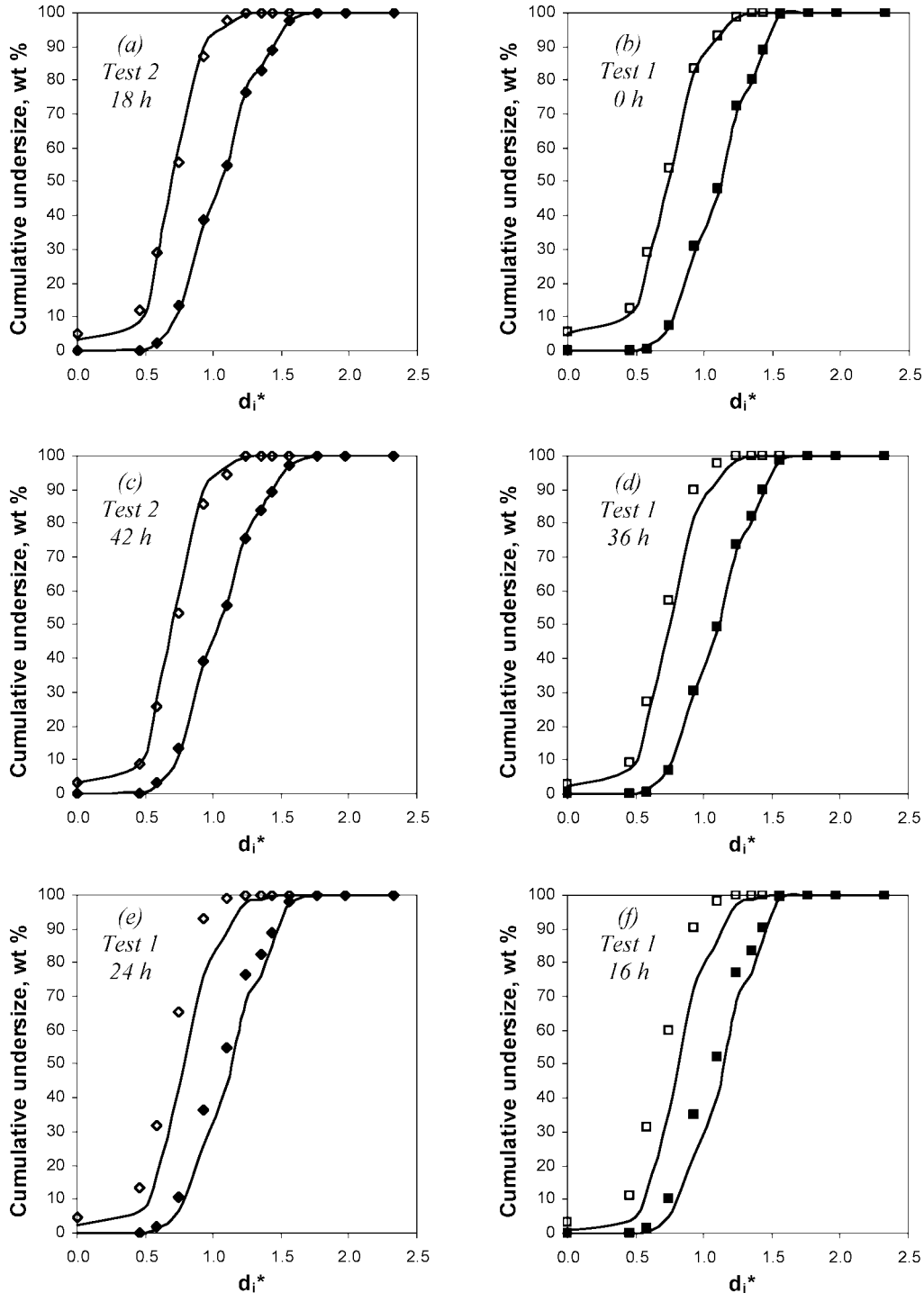

Figure 7. Selected experimental and predicted size distributions for the bottom deck. Screen A: (◆) experimental oversize, (◇) experimental undersize, and (—) predicted. Screen B: (■) experimental oversize, (□) experimental undersize, and (—) predicted.

and f, correspond to the calculated PSDs that most deviate from the experimental ones for screens A and B, respectively. Considering the relatively high number of experimental points (i.e., 468, 18 samples × 13 classes × 2 screens) to be reproduced for each stream (i.e., undersize and oversize) by estimating only three parameters, it can be concluded that the goodness of the fitted model is satisfactory. In fact, for the oversize stream, 75% of the calculated points have less than 5% of error, 81% less than 10%, and 92% less than 20%. For the undersize stream the results are even better: 97.7% of the data are within 5% of error, 98.8% within 10%, and 99.6% within 20%.

Figure 7 presents some selected experimental and calculated PSDs of the oversize (P) and undersize streams (U) for the bottom decks of screens A and B. The oversize corresponds to the product stream and the undersize to the fraction of fines recycled directly from the double-deck screens to the granulator. Again, three distributions from each screen are shown, Figure 7e,f being representative of the worst results. Regarding these bottom decks, 84% of the calculated points for the oversize stream have less than 30% error and for the undersize stream 81% have less than 30% error. In general, the fitting is not as good as that obtained for the top deck. Nevertheless, and taking into account the errors inherent to sample collection, it can be considered to be in reasonable agreement with the experimental data.

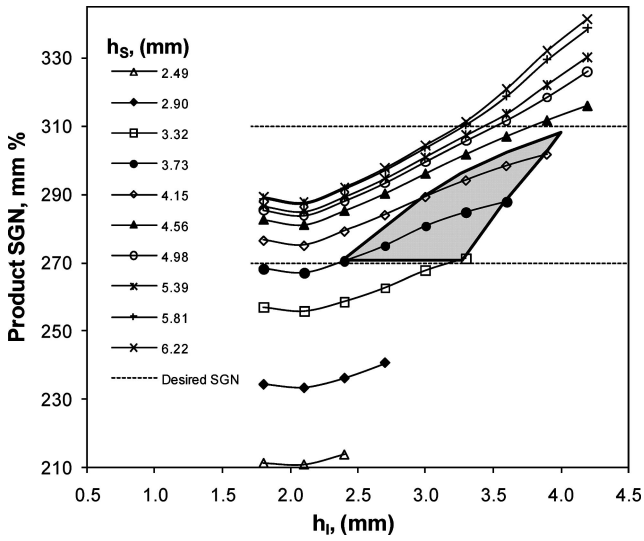

Figure 8. Influence of the upper (h_S) and lower (h_I) deck apertures on the product SGN. Constant product mass flow rate.

From an industrial point of view, it is interesting to determine the effect of the top and bottom decks screen apertures (h_S and h_I, respectively) on the product quality and recycle ratio. With this aim, different simulations were performed. It is difficult to explore the screens performance within the whole granulation circuit because changes in one parameter influence all the other circuit parameters, leading to another screen feed mass flow and different PSDs. To get a qualitative idea of the effect of h_S and h_I on the screen operation, a given feed composition (specifically, the one reported in Figure 5) is chosen.[14]

Two parameters are commonly used in the fertilizers industry to define the product quality. The size guide number (SGN) represents the particle size in millimeters for which 50% by weight of the product is coarser and 50% is finer, multiplied by 100. The uniformity index (UI) characterizes the spread of the product particle size distribution and is defined as the ratio of the opening size that would retain 95% of the corresponding sample to the opening that would retain 10%, multiplied by 100. For the special case of granulated urea production, values of UI greater than 50 and SGN in between 270 and 310 are suggested.[35−37] Furthermore, the product size is preferred to be within the range 2−4 mm.[35] For this reason, the screen apertures were modified from 2.5 to 6.2 mm for the top deck and from 1.8 to 4.2 mm for the bottom deck, considering as unfeasible those combinations that gave h_I greater than or equal to h_S. The product mass flow was kept constant for all the simulations that were carried out.

Figure 8 shows the dependency of the product SGN with both deck apertures. The desired region (270−310) is reached as both h_S and h_I increase, provided $h_I < h_S$ and h_S is not so high as to give values of SGN greater than those required. Higher top and lower deck apertures allow the passage of bigger particles to the product stream and a lesser amount of fines, respectively, resulting in higher SGN values.

Figure 9 shows the influence of both screen apertures on the product UI. As it can be seen, the desired uniformity index region is reached as h_S decreases and h_I increases, as long as $h_I < h_S$. Under the desired region, the UI parameter shows greater variations for changes in the aperture of the top deck than for those corresponding to the bottom one. Nevertheless, as the h_S values become higher, this sensitivity is less strong since the oversize stream becomes practically zero.

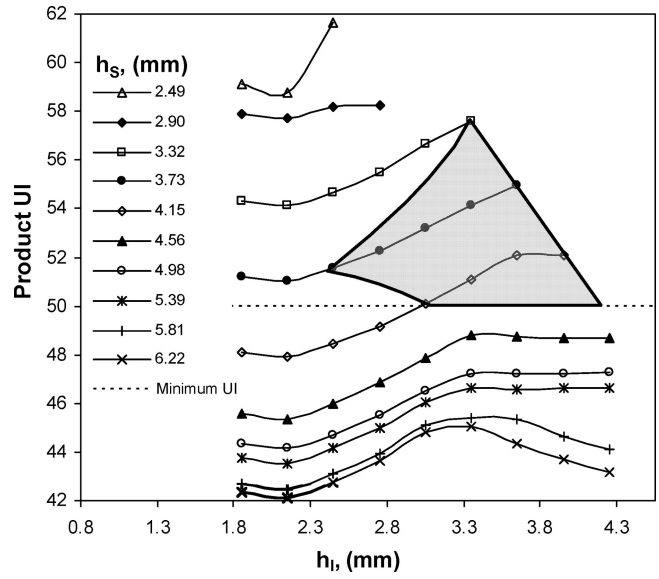

Figure 9. Influence of the upper (h_S) and lower (h_I) deck apertures on the product UI. Constant product mass flow rate.

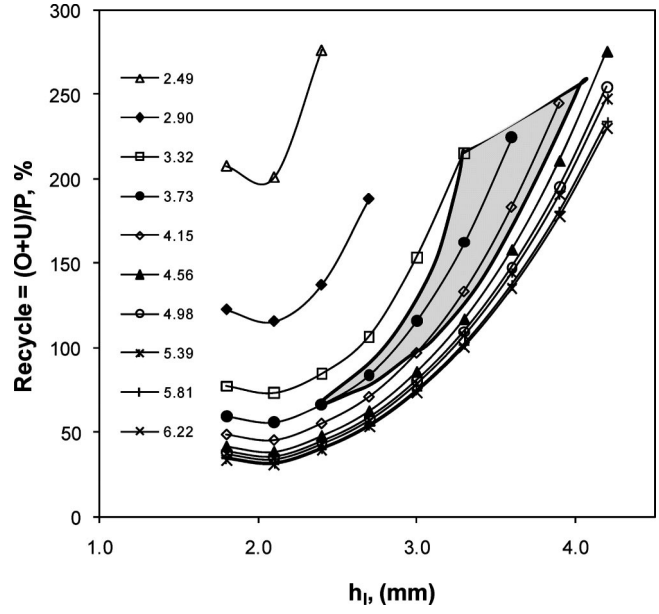

Figure 10. Influence of the upper (h_S) and lower (h_I) deck apertures on the screens' recycle ratio. Constant product mass flow rate.

Figure 10 shows the effect of the screen apertures on the recycle ratio. The recycle is defined as the amount of material out of specification that returns to the production circuit as seeds for the granulation unit. It involves the fines and oversize streams from the screens. In terms of the feed and product streams, the recycle ratio is

$$\text{recycle ratio} = 100\frac{F-P}{P} = 100\frac{O+U}{P} \qquad (14)$$

As the top deck aperture decreases and the bottom deck aperture increases, the feed necessary to produce the same amount of product flow rate increases and thus a greater recycle ratio results. Over a certain h_S value, the amount of oversize becomes close to zero and practically does not affect the recycle.

As expected, the effects of the screen apertures on the product UI and recycle ratio are opposite. If narrower product PSDs are required, higher undesired recycle ratios are obtained.

Therefore, once the appropriate lower and upper deck apertures have been set in order to fulfill the product UI and SGN requirements, the possible recycle ratios should be analyzed to determine the feasibility of the chosen set of screens apertures. As an example, the shaded areas in Figures 8−10 represent the h_S and h_I combinations that allow satisfying the UI and SGN urea specifications simultaneously. The recycle ratio is strongly affected by the mesh apertures. Thus, the optimal combinations of deck apertures are determined by the maximum acceptable recycle ratios.

7. Conclusions

The fitted Karra[1] model, which allows successful estimation of the experimental d_{50} values, reproduces in an accurate way the mass flow and particle size distributions of all the solid streams that leave the large-scale urea screens (undersize, oversize, and product fractions) for different feed PSDs and mass flow rates.

The presented fitted parameters together with the Karra[1] model can be used in urea granulation circuit simulators for many existing plants, which (independently of the technology) have similar industrial vibrating double-deck screens to attain the marketable product granulometry.

The simulation results indicate that the screen apertures of both decks have a decisive influence on the recycle ratio values and consequently on the performance of the granulation circuit. It was found that the feasible top and bottom deck apertures, which maintain the product quality and recycle ratio within the desired limits, are constrained to a very narrow size range. Therefore, the screen model can be also used as a design tool or to explore new screen apertures combinations for granulation plant revampings.

Acknowledgment

The authors express their gratitude for the financial support by the Consejo de Investigaciones Científicas y Técnicas (CONICET), Agencia Nacional de Promoción Científica y Tecnológica (ANPCyT), and Universidad Nacional del Sur (UNS) of Argentina.

Notation

A = screen basic capacity (ton/h m^2)
$a = d_{50}$ exponent
B = factor for % of oversize in the screen feed
C = factor for % of half-size under in the screen feed
D = factor for deck location
d_i = geometric mean particle size, $[(d_1 d_2)_i]^{1/2}$(mm)
d_i^* = dimensionless geometric mean particle size, d_i/d_{50}^F
d_1 = lower limit for size class i (mm)
d_2 = upper limit for size class i (mm)
d_{50} = cut size, particle size corresponding to the 50% of the partition curve (mm)
d_{50}^F = cut size of the feed shown in Figure 5 (mm)
E = factor for wet screening
E_p = Ecart probability or probable error $E_P = (d_{75} - d_{25})/2$ (mm)
F = total feed stream to the screens (ton/h)
F_A = feed stream to screen A (ton/h)
F_B = feed stream to screen B (ton/h)
F_D = bulk density factor
f_0 = objective function of the data reconciliation problem
G = factor for % of near size in the screen feed
h = screen aperture (mm)
h_I = lower deck screen aperture (mm)
h_S = upper deck screen aperture (mm)
i = size class index
j = screen substream index
K = correction parameter (ton/(h m^2))
L = deck location; top = 1, second = 2, etc.
M = number of streams around the screens with different particle size distributions
m = Plitt's adjustable parameter; classification sharpness
N = number of experimental points for data reconciliation
O = total oversize stream from the screens (ton/h)
O_A = oversize stream from screen A (ton/h)
O_B = oversize stream from screen B (ton/h)
P = total product stream from the screens (ton/h)
P_A = product stream from screen A (ton/h)
P_B = Product stream from screen B (ton/h)
Q = % of oversize material in feed to deck
R = % of half-size material in feed to deck
S = screen surface (m^2)
SGN = size guide number, $100 d_{50}$ (mm %)
$T = 1.26h$
T_i = oversize partition coefficient for each size class i
U = total undersize stream from the screens (ton/h)
U_A = undersize stream from screen A (ton/h)
U_B = undersize stream from screen B (ton/h)
UI = uniformity index, $100 d_{95}/d_{10}$
U^T = theoretical undersize mass flow fed to the screen (ton/h)
W_{ji} = variance associated with the experimental samples
X = % of near-mesh material in feed to deck
$X_{F_A i}$ = mass fraction of each size class in feed to screen A
$X_{F_B i}$ = mass fraction of each size class in feed to screen B
$X_{O_A i}$ = mass fraction of each size class in oversize from screen A
$X_{O_B i}$ = mass fraction of each size class in oversize from screen B
$X_{P_A i}$ = mass fraction of each size class in product from screen A
$X_{P_B i}$ = mass fraction of each size class in product from screen B
$X_{U_A i}$ = mass fraction of each size class in undersize from screen A
$X_{U_B i}$ = mass fraction of each size class in undersize from screen B
$\overline{X_{ji}}$ = average mass fraction of experimental samples for size class i and substream j
X_{ji} = estimated mass fraction of the experimental samples for size class i and substream j

Greek Notation

λ = screens feed split coefficient
ρ_B = bulk density (kg/m^3)

Literature Cited

(1) Karra, V. K. Development of a Model for Predicting the Screening Performance of a Vibrating Screen. *CIM Bull.* **1979**, *72* (804), 167–171.

(2) Adetayo, A. A.; Litster, J. D.; Cameron, I. T. Steady State Modeling and Simulation of a Fertilizer Granulation Circuit. *Comput. Chem. Eng.* **1995**, *19*, 383–393.

(3) Liu, L. X.; Litster, J. D. Population Balance Modelling of Granulation with a Physically Based Coalescence Kernel. *Chem. Eng. Sci.* **2002**, *57*, 2183–2191.

(4) Tan, H. S.; Goldschmidt, M. J. V.; Boerefijn, R.; Hounslow, M. J.; Salman, A. D.; Kuipers, J. A. M. Population Balance Modelling of Fluidized Bed Melt Granulation, An Overview. *Chem. Eng. Res. Des.* **2005**, *83*, 871–880.

(5) Balliu, N. E. "An Object Oriented Approach to the Modeling and Dynamics of Granulation Circuits". Ph.D. Thesis, University of Queensland, Australia, 2005.

(6) Heffer, P.; Prud'Homme, M. Outlook for World Fertilizer Demand, Supply, and Supply/Demand Balance. *Turk. J. Agric. Forestry* **2008**, *32*, 159–164.

(7) Korotkiy, I.; Brazgovka, A.; Kremers, G. Urea Granulation Experience. Presented at the Tenth Stamicarbon Urea Symposium, 2004.

(8) Bertin, D. E.; Mazza, G. D.; Piña, J.; Bucalá, V. Modeling of an Industrial Fluidized Bed Granulator for Urea Production. *Ind. Eng. Chem. Res.* **2007**, *46*, 7667–7676.

(9) Cotabarren, I.; Schulz, P. G.; Bucalá, V.; Piña, J. Modeling of an Industrial Double Roll Crusher of a Urea Granulation Circuit. *Powder Technol.* **2008**, *183* (2), 224–230.

(10) Heinrich, S.; Peglow, M.; Mörl, L. Particle Population Modeling in Fluidized Bed Spray Granulation - Analysis of the Steady State and Unsteady Behavior. *Powder Technol.* **2003**, *130*, 154–161.

(11) Zhang, J.; Litster, J. D.; Wang, F. Y.; Cameron, I. T. Evaluation of Control Strategies for Fertilizer Granulation Circuits Using Dynamic Simulation. *Powder Technol.* **2000**, *108*, 122–129.

(12) Drechsler, J.; Peglow, M.; Heinrich, S.; Ihlow, M.; Mörl, L. Investigating the Dynamic Behavior of Fluidized Bed Spray Granulation Processes Applying Numerical Simulation Tools. *Chem. Eng. Sci.* **2005**, *60*, 3817–3833.

(13) Radichkov, R.; Müller, T.; Kienle, A.; Heinrich, S.; Peglow, M.; Mörl, L. A Numerical Bifurcation Analysis of Continuous Fluidized Bed Spray Granulation with External Product Classification. *Chem. Eng. Process.* **2006**, *45*, 823–837.

(14) Wildeboer, W. J. "Steady State and Dynamic Simulations of a Closed Loop Granulation Circuit". Master's Thesis, Delft University of Technology, The Netherlands, 1998.

(15) Li, J.; Webb, C.; Pandiella, S. S.; Campbell, G. M. Discrete Particle Motion on Sieves, a Numerical Study Using the DEM Simulation. *Powder Technol.* **2003**, *133*, 190–202.

(16) Whiten, W. J. "Simulation and Model Building for Mineral Processing". Ph.D. Thesis, University of Queensland, Australia, 1972.

(17) Ferrara, G.; Preti, U.; Schena, G. D. Modelling of Screening Operations. *Int. J. Miner. Process.* **1988**, *22*, 193–222.

(18) Subasinghe, G. K. N. S.; Schaap, W.; Kelly, E. G. Modelling the Screening Process: A Probabilistic Approach. *Powder Technol.* **1989**, *59*, 37–44.

(19) Subasinghe, G. K. N. S.; Schaap, W.; Kelly, E. G. Modelling the Screening Process as a Conjugate Rate Process. *Int. J. Miner. Process.* **1990**, *28*, 289–300.

(20) Soldinger, M. Interrelation of Stratification and Passage in the Screening Process. *Miner. Eng.* **1999**, *12* (5), 497–516.

(21) Wills, B.; Napier-Munn, T. *Will's Mineral Processing Technology, Seventh Edition: An Introduction to the Practical Aspects of Ore Treatment and Mineral Recovery*; Butterworth-Heinemann: London, 2006.

(22) *Aspen Plus 12.1. Unit Operation Models*; Aspen Technology Inc.: Cambridge, MA, June 2005.

(23) *Modsim Simulator*; Mineral Technologies Inc.: Salt Lake City, UT; http://www.mineraltech.com/MODSIM.

(24) *Moly-Cop Tools*; Moly-Cop Chile S.A.: Santiago, Chile; http://www.molycop.cl.

(25) Adetayo, A. A. "Modelling and Simulation of the Fertilizer Granulation Circuit". Ph.D. Thesis, University of Queensland, Australia, 1993.

(26) Molerus, O.; Hofmann, H. Darstellung von Windsichterkurven durch ein stochastisches Modell. *Chem. Ing. Tech.* **1969**, *41* (5/6), 340–344.

(27) Reimers, C.; Werther, J.; Gruhn, G. Flowsheet Simulation of Solids Processes: Data Reconciliation and Adjustment of Model Parameters. *Chem. Eng. Process.* **2008**, *47*, 138–158.

(28) Standish, N.; Bharadwaj, A. K.; Hariri-Akbari, G. A Study of the Effect of Operating Variables in the Efficiency of a Vibrating Screen. *Powder Technol.* **1986**, *48*, 161–172.

(29) Allen, T. *Particle Size Measurement I: Powder sampling and particle size measurement*, 5th ed.;Chapman & Hall: London, 1997.

(30) *Athena Visual Studio, Software for Modeling and Parameter Estimation*; Athena Visual Software, Inc., Naperville, IL; http://www.AthenaVisual.com.

(31) King, R. P. *Modeling and Simulation of Mineral Processing Systems*; Butterworth-Heinemann: Oxford, UK, 2001.

(32) *Nordberg Process Machinery: Reference Manual*, Renox, 1st ed., 1976.

(33) Plitt, L. R. The Analysis of Solid-Solid Separations in Classifier. *CIM Bull.* **1971**, *64*, 42–47.

(34) Gupta, A.; Yan, D. *Mineral Processing Design and Operations*; Elsevier: Dordrecht, The Netherlands, 2006.

(35) Karnaphuli Fertilizer Co. Ltd., Rangadia, Anowara Chittagong, Bangladesh; http://www.kafcobd.com/html/products.html.

(36) CF Industries, Deerfield, IL. http://cfindustries.com/producturea.htm.

(37) The Franco Chiesa SPA Italian Commodities Trading Department; http://www.chiesa.it/urea.htm.

Received for review June 19, 2008
Revised manuscript received November 11, 2008
Accepted January 2, 2009

IE800968Y